Screening of potential inhibitors for COVID-19 main protease from phytoconstituents of *Tectona grandis* Linn: application of molecular modeling studies

Anoop K
School of Lifesciencess, Kannur University https://orcid.org/0000-0002-9613-3259
Varun T K
School of Lifesciencess, Kannur University
Ajeesh A K
School of Lifesciencess, Kannur University
Aravind A
School of Lifesciencess, Kannur University
Muhammad Azharuddin M
School of Lifesciencess, Kannur University
Praveen P
School of Lifesciencess, Kannur University
Sayeed Ali M P
School of Lifesciencess, Kannur University
Jayadevi Variyar E (ejayadevi@gmail.com)
School of Lifesciencess, Kannur University

Research Article

Keywords: Novel Coronavirus, COVID-19, Protease, Molecular Docking, Tectona grandis Linn

Posted Date: April 7th, 2020

DOI: https://doi.org/10.21203/rs.3.rs-21617/v1

Abstract

The recent outbreak of novel coronavirus disease, COVID-19 has created a threat to human population across the world. The unavailability of specific therapeutics and vaccines, demands the sincere efforts in this direction. Main Proteases of this novel Coronavirus (SARS-CoV-2) play critical role during the disease propagation, and hence represents a crucial target for the drug discovery. Reported phytoconstituents of *T. grandis* Linn were prepared for docking evaluation. The current objective of the study is to identify some naturally occurring product from *Tectona grandis* Linn. and evaluate its binding activity against COVID-19 Major protease as novel Coronavirus (SARS-CoV-2) target through in silico docking studies. The study results showed that all the selected phytoconstituents showed binding energy ranging between -7.723 to -1.524 kcal/mol. Barleriaquinone-I exhibited highest binding affinity -7.723 Kcal/mol and strong, stable interactions with the amino acid residues present on the active site of COVID-19 Main Protease. Our findings suggest that these phytoconstituents molecules can be used as potential inhibitors against COVID-19 Main Protease. However, further investigation and validation of these inhibitors against SARS-CoV-2 are needed to claim their candidacy for clinical trials

1. Introduction

Medicinal plants have been widely used to treat a wide variety of infectious as well as non- infectious ailments. Many of the plant derived compounds exhibit antiviral properties and are found to be effective against various viral infections. Due to their low toxicity and possible multi- step mechanism, which means, lesser selective pressure for the emergence of resistant strains, natural products have been encouraged for searching new drugs. In addition, the majority of the compounds used for the clinical purpose are targeted for a diminutive number of viruses. (De Clercq, 2004) Ethnopharmacological screenings of the medicinal plants have shown that a vast number of phytochemicals such as alkaloids, anthraquinones, coumarins, flavonoids, polyphenols, tannins, terpenoids, among others, are active against virus. (Hupfeld and Efferth, 2009)The antiviral activity of the natural compounds may occur by inhibition of one or more steps of viral replication. By direct interaction with the viral particle, they can prevent infection; change of the adsorption venture by official to cell receptors; hindrance of infection infiltration into the host cell, by viewing for pathways of actuation of intracellular signs, and all the more regularly, meddling with various phases of viral replication (Ghosh et al., 2009). Coronaviruses (CoVs) are the family of viruses containing single-stranded RNA (positive-sense) which is encapsulated by a membrane envelope. They are classified in the Nidovirales order, Coronaviridae family, which is comprised of two sub-families and about 40 known species. These species are divided and characterized into four gene era (alpha, beta, gamma and delta), and only the alpha and beta- strains are identified to be pathogenic to human and other mammals (Y. Chen et al., 2020; Paules et al., 2020) Before 2019, six coronaviruses were known to cause respiratory and enteric diseases in humans, especially the two of them belonging to betaviruses cause severe illness: SARS (Severe Acute Respiratory Syndrome)-CoV and MERS (Middle East Respiratory Syndrome)-CoV. (Hui et al., 2020; Song et al., 2019). On 7 January 2020, a new coronavirus, 2019-nCoV (now officially named SARS-CoV-2) was implicated in an alarming outbreak

of a pneumonia-like illness COVID–19, originating from Wuhan City, Hubei, China. Human-to-human transmission was first confirmed in Guangdong, China (Y. W. Chen et al., 2020). The World Health Organization has declared global public health emergency on 4 March 2020 as there are more than 90,000 confirmed cases reported, and the death toll is over 3000. In the height of the crisis, this virus is spreading at a rate and scale far worse than previous coronaviral epidemics. Coronaviruses possess extraordinarily large single- stranded RNA genomes—approximately 26 to 32 kilo bases in length. This genome acts just like a messenger RNA when it infects a cell, and directs the synthesis of two long polyproteins that include the machinery that the virus needs to replicate new viruses. These proteins include a replication/transcription complex that makes more RNA, several structural proteins that construct new virions, and two proteases. The proteases play essential roles in cutting the polyproteins into all of these functional pieces. It is a dimer of two identical subunits that together form two active sites. The protein fold is similar to serine proteases like trypsin, but a cysteine amino acid and a nearby histidine perform the protein-cutting reaction and an extra domain stabilizes the dimer. This structure has a peptide-like inhibitor bound in the active site (Cui et al., 2019; St John et al., 2015). Bioinformatics is one of the most important and innovative approaches in the design and manufacture of new drugs. Since the clinical and laboratory trials are costly and tedious in nature, various bioinformatics techniques are nowadays used for designing new drugs. Molecular docking, simulation, target point determination and chemical stability studies are the most important bioinformatics methods used in drug design. In the meantime, molecular docking has a special place in the process of designing new drugs, examining and comparing their efficacy (Grinter and Zou, 2014; Mukesh and Rakesh, 2011).

Tectona grandis Linn (Teak), is locally known as Sagwan, belongs to Lamiaceae family. It is one of the most valuable timber in the world, due to its beautiful surface and its resistance to termite and fungal damage. The main active ingredient compounds that are responsible for these action are tectoquinone, lapachol and deoxylapachol. Naphthoquinones, anthraquinones and isoprenoid quinones are abundant metabolites in teak. In addition to these, teak contains several other phytochemicals such as triterpenoids, steroids, lignans, fatty esters and phenolic compounds. Pharmacologically, the plant has been investigated for antioxidant, anti-inflammatory, anti- pyretic, cytotoxic, analgesic, hypoglycemic, wound healing and antiplasmodial activities. Based on the above view, the aim of our study is to identify some naturally occurring product and evaluate its binding activity against against COVID–19 major protease through *in silico* molecular docking studies.

2. Methods

Glide docking uses the hypothesis of a rigid receptor although scaling of van der Waals radii of nonpolar atoms, which decreases penalties for close contacts, can be used to model a slight “give” in the receptor and/or ligand. Docking studies of designed compounds were carried out using grid-based ligand docking with energetics (GLIDE) module version 5.9. Schrödinger, LLC, New York, NY, 2013. The software package running on multiprocessor Linux PC. GLIDE has previously been validated and applied successfully to predict the binding orientation of many ligands.

Data sources

In this study, a dataset of active phytochemicals were obtained from FDA and Indian Medicinal Plants, Phytochemistry, and Therapeutics and pubchem database.

Protein structure preparation

The X-ray crystal structures of COVID–19 major protease (PDB: 6LU7) (Prajapat et al., 2020) retrieved from the RCSB Protein Data Bank (*https://www.rcsb.org/structure/6LU7)* PDB is an archive for the crystal structures of biological macromolecules, worldwide (Jayaprakasha et al., 2002). Water molecules of crystallization were removed from the complex, and the protein was optimized for docking using the protein grounding and refinement utility provided by Schrödinger LLC.

Determination of Active Sites

The amino acids in the active site of a protein were determined using the Computed Atlas for Surface Topography of Proteins (CASTp) (http://sts.bioe.uic.edu/castp/index.html?201l) and Biovia Discovery Studio 4.5. The determination of the amino acids in the active site was used to analyze the Grid box and docking evaluation results. Discovery Studio is an offline life sciences software that provides tools for protein, ligand, and pharmacophore modelling (Gopal Samy and Xavier, 2015).

Target protein and ligand preparation

The structures of energetic constituents of *T. Grandis* were constructed by means of the splinter dictionary of Maestro 9.3 (Schrodinger, LLC) using the optimized potentials for liquid simulations-all atom force field with the steepest descent followed by curtailed Newton conjugate gradient protocol. The crystal structure of the above-mentioned targets was downloaded from the Protein Data Bank (PDB) and Pubchem databases. The selected protein targets were prepared for docking studies using the protein preparation wizard module in Schrodinger program (Maestro 9.3.). The preparation includes force field parameters assignment, energy minimization and H-bond assignment. The energy minimized models of ligands obtained after molecular modeling studies were then prepared using ligprep module. Geometries of ligands was optimized using OPLS–2005 force field and ionization generates possible states at target pH 7.0 ± 2.0

Receptor Grid preparation and Molecular Docking

All docking calculations were performed using the “extra precision” mode of GLIDE program. A receptor grid that defines the specific area of the protein to which the interaction of ligand has to be tested was defined by the receptor grid generation module. The position of the co- crystal ligand defines the Centre of the grid For the binding site, an assortment of energy grids was premeditated and stored, is distinct in terms of two concentric cubes: The bounding box, which must contain the center of any satisfactory ligand pose, and the enclosing box, which must contain all ligand atoms of an satisfactory pose, with a root mean square deviation of <0.5 Å and a maximum atomic displacement of <1.3 Å were eliminated as unneeded to increase assortment in the retained ligand poses. The scale factor for van der Waals radii was applied to those atoms with absolute partial charges ≤0.15 (scale factor of 0.8) and 0.25 (scale factor of 1.0) electrons for ligand and protein, respectively. Energy minimization protocol includes

dielectric constant of 4.0 and 1000 steps of conjugate gradient. Upon end of each docking calculation, for the most part, 100 poses per ligand were generated. The most excellent docked structure be preferred using a GLIDE score (G-score) function (Amudha and Rani, 2016; Parasuraman et al., 2014)

Glide Score = 0.065*vdW + 0.130*Coul + Lipo + Hbond + Metal + BuryP + RotB + Site

Analysis and visualization
Visual analysis of the docking site was performed using Pymol version 2.3.4 and the results were validated using Schrodinger program (Maestro 9.3.)

ADME analysis
On the basis of canonical SMILES of the selected ligands obtained from pubchem, ADME properties of the studied compound were calculated using online Swiss ADME program. The major parameters for ADME associated properties such as Lipinski's rule of five, the solubility of the drug, pharmacokinetic properties and drug likeliness were considered. The values of the observe properties are presented in Table 3.

3. Results And Discussion

Coronaviruses (CoVs) are the family of viruses containing single-stranded RNA (positivesense) which is encapsulated by a membrane envelope. They are classified in the Nidovirales order, Coronaviridae family, which is comprised of two sub-families and about 40 known species. These species are divided and characterized into four gene era (alpha, beta, gamma and delta), and only the alpha and beta- strains are identified to be pathogenic to human and other mammals. Bioinformatics is one of the most important and innovative approaches in the design and manufacture of new drugs. Due to the high cost of clinical and laboratory trials, the time consuming and the possibility of error, various bioinformatics techniques are nowadays used in the design of new drugs. Molecular docking, simulation, target point determination and chemical stability studies are the most important bioinformatics methods used in drug design. In the meantime, molecular docking of a special place in the process of designing new drugs, examining and comparing their efficacy enjoyable (Grinter and Zou, 2014; Mukesh and Rakesh, 2011). One of the novel therapeutic strategies for virus infection apart from the design and chemical synthesis of protease inhibitors is the search for inhibitors of this enzyme among natural compounds in order to obtain drugs with minimal side effects. *T. grandis* has variety of medicinal properties and traditional uses. Virtually every part of the teak tree has medicinal properties. The decoction of bark is used in bronchitis, hyperacidity, dysentery, verminosis, burning sensation, diabetes, difficult labor, leprosy and skin diseases (Vyas et al., 2019). It is important to know that, which secondary plant metabolites are found in plant as it may provide a basis for its traditional uses. During more than 100 years of intensive research on the chemistry of *T. grandis,* various compounds have been detected from different parts of the plant includes Quinones are major secondary metabolites and other common phytochemicals (Table 1). The figure 1–7 shows the structures of the compounds that identified from the plant and selected for the *in silico* studies.

Table 1: Compounds isolated from *T. grandis*.

Compound name (Molecular formula)	Plant part & References
NAPHTHOQUINONES	
1.Lapachol(C15H14O3)	Heartwood (GUPTA and SINGH, 2004; Martin et al., 1974)
2.Deoxylapachol (C15H14O2)	Heartwood (Burnett and Thomson, 1967; Gupta and Singh, 2004)
3. 5-Hydroxylapachol (C15H14O4)	Root heartwood (Khan and Mlungwana, 1999)
4. 4. Hydroxysesamone (C15H14O5)	Leaves (Kopa et al., 2014)
5. α-Lapachone (C15H14O3)	Roots (Krishna et al., 1977)
6. β-Lapachone (C15H14O3)	Roots (Krishna et al., 1977)
7. Dehydro- α -lapachone (C15H12O3)	Heartwood (Gupta and Singh, 2004)
8. 4’5’-Dihydroxy-epiisocatalponol (C15H18O4)	Heartwood (Mounguengui et al., 2016)
9. Tectol (C30H26O4)	Heartwood (Lukmandaru and Takahashi, 2009)
10. Dehydro-α-isodunnione (C15H12O3)	Heartwood (Gupta and Singh 2004)
11. Tecomaquinone-I (C30H24O4)	Heartwood (Gupta and Singh, 2004)
ANTHRAQUINONES	
12. Tectoquinone (C15H10O2)	Heartwood (Sandermann and Simatupang, 1966)

13. 2-Hydroxymethyl-anthraquinone (C15H10O3)	(Windeisen et al., 2003)
14. 2-Acetoxymethyl-anthraquinone (C15H12O4)	Heartwood (Rudman, 1960)
15. Anthraquinone-2-carbaldehyde (C15H8O3)	Heartwood (Rudman, 1960)
16. Anthraquinone-2-carboxylic acid (C15H8O4)	Heartwood (Rudman, 1960)
17. 3-Hydroxy-2-methyl-anthraquinone (C15H10O3)	Heartwood (Kopa et al., 2014)
18. Pachybasin (C15H10O3)	Heartwood (Thomson, 2012)
19. Rubiadin (C15H10O4)	Heartwood (Burnett and Thomson, 1968)
20. Munjistin (C15H8O6)	Heartwood (Burnett and Thomson 1968) Roots (Joshi et al.1977)
21. 2-Methylquinizarin (C15H10O4)	Heartwood (Sandermann and Simatupang 1966) Root (Khan and Mlungwana 1999)
22. Quinizarine (C14H8O4)	Leaves (Kopa et al. 2014)
23. 1-Hydroxy-2-methyl anthraquinone (C15H10O3)	Stem (Windeisen et al. 2003)
24. 5,8-dihydroxy-2-methylanthraquinone (C15H10O4)	Leaves (Kopa et al. 2014)
25. Obtusifolin (C16H12O5)	Saw dust (Sumthong et al., 2008)
26. 9,10-Dimethoxy-2-methyl-1,4-anthraquinone(C17H14O4)	Heartwood (Singh et al., 1989)
27. 5-Hydroxy-2-methyl anthraquinone (C15H10O3)	Heartwood (Agarwal et al., 1965)
28. 1-Hydroxy-5-methoxy-2-methylanthraquinone(C16H12O4)	Heartwood (Agarwal et al., 1965)
29.1,5-Dihydroxy-2methylanthraquinone (C15H10O4)	Heartwood (Agarwal et al., 1965)
30. 5-Hydroxydigitolutein (C16H12O5)	Tissue culture (Dhruva et al., 1972)
31. Barleriaquinone-I (C15H10O3)	Heartwood (Singh et al. 2008)
32. Tectoleafquinone (C19H14O6)	Leaves (Agarwal et al., 1965)
33. Grandiquinone A (C17H12O5)	Leaves (Kopa et al. 2014)
34. Tectograndone (C30H20O10)	Leaves (Kopa et al. 2014)
35. Anthratectone (C27H18O9)	Leaves (Lacret et al., 2011)
36. Naphthotectone (C17H16O7)	Leaves (Lacret et al., 2011)
MONOTERPENE	
37. (6RS)-(E)-2,6-Dimethyl-2,7-octadiene-1,6-diol (C10H18O2)	Leaves (Macias et al. 2008)

SESQUITERPENES	
38. lβ-6-α-Dihydroxy-4(15)-eudesmene (C15 H26O2)	Leaves and Bark (Macias et al.2010)
39. 7-Epieudesm-4(15)-ene-1α,6α-diol (C15 H26O2)	Leaves and Bark (Macias et al. 2010)
DITERPENES	
40. Abeograndinoic Acid (C20H32O4)	Leaves and Bark (Macias et al. 2010)
41. Phytol (C20H40O)	Leaves and Bark (Macias et al. 2010)
42. 7,11,15-Trimethyl-3-methylene-hexadecan-1,2-diol (C20H40O2)	Leaves and Bark (Macias et al. 2010)
43. Rhinocerotinoic acid (C20H30O3)	Leaves and Bark (Macias et al. 2010)
44. 2-Oxokovalenic acid (C20H30O3)	Leaves and Bark (Macias et al. 2010)
45. 19-Hydroxyferruginol (C20H30O2)	Leaves and Bark (Macias et al. 2010)
46. Tectograndinol (C20H34O3)	Leaves (Horst and Ilona 1977)
47. Solidagonal acid (C20H30O3)	Leaves and Bark (Macias et al. 2010)
TRITERPENES	
48. Lupeol (C30H50O)	Bark (Pathak et al. 1988)
49. Betulin (C30H50O2)	Bark (Pathak et al. 1988)
50. Betulinaldehyde (C30H48O2)	Bark (Pathak et al.1988)
51. Betulinic acid (C30H48O3)	Heartwood and Stem bark (Sandermann and Simatupang 1966; Khan et al. 2010) Bark (Ahluwalia and Seshadri 1957) Roots (Dayal and Seshadri 1979) Leaves (Kopa et al. 2014)
52. Ursolic acid (C30H48O3)	Leaves (Kopa et al. 2014); Bark (Macias et al. 2010)
53. Corosolic acid (C30H48O4)	Leaves (Kopa et al. 2014)
54. Oleanolic acid (C30H48O3)	Leaves and Bark (Macias et al. 2010)
55. Maslinic acid (C30H48O4)	Leaves and Bark (Macias et al. 2010)
56. Methyl-2α,3α-dihydroxyurs-l2-en-28-oate (C30H48O4)	Leaves and Bark (Macias et al. 2010)
57. Euscaphic acid (C30H48O5)	Leaves and Bark (Macias et al. 2010)
58. Squalene (C30H50)	Roots (Windeisen et al. 2003; Khan and Mlungwana 1999
POLYTERPENE OR RUBBER	

59. Caoutchouc or Indian rubber Polymer	Wood (Sandermann and Dietrichs 1959; Narayanamurti and Singh 1960; Yamamoto et al. 1998)
APOCAROTENOIDS	
60. Tectoionol A ($C_{13}H_{23}O_3$)	Leaves (Macías et al., 2008)
61. Tectoionol B ($C_{13}H_{24}O_2$)	Leaves (Macias et al. 2008)

62. Annuionone D (C13H20O3)	Leaves (Macias et al. 2008)
63. 3β-Hydroxy-7,8-dihydro-β-ionol (C13H24O2)	Leaves (Macias et al. 2008)
64. 9(S)-4-Oxo-7,8-dihydro-β-ionol (C13H22O2)	Leaves (Macias et al. 2008)
65. 3β-Hydroxy-7,8-dihydro-β-ionone (C13H22O2)	Leaves (Macias et al. 2008)
PHENOLIC COMPOUNDS	
66. Gallic acid (C7H6O5)	Leaves (Nayeem and Karvekar, 2010)
67. Ellagic acid (C14H6O8)	Leaves (Nayeem and Karvekar 2010)
68. Acetovanillone (C9H10O3)	Leaves (Lacret et al. 2012)
69. E-Isofuraldehyde (C10H10O3)	Leaves (Lacret et al. 2012)
70. 3-Hydroxy-1-(4-hydroxy-3,5-dimethoxyphenyl) propan-1-one (C11H14O5)	Leaves (Lacret et al. 2012)
71. Evofolin A (C17H1806)	Leaves (Lacret et al. 2012)
FLAVONOIDS	
72. Rutin (C27H30O16)	Leaves (Nayeem and Karvekar 2010)
73. Quercitin (C15H10O7)	Leaves (Nayeem and Karvekar 2010)
STEROIDS/ SAPONINS	
74. β-Sitosterol (C29H50O)	Roots (Joshi et al. 1977; Dayal and Seshadri 1979)
75. Hydroxyenone (C29H48O2)	Leaves and Bark (Macias et al. 2010)
76. β-Sitosterol-β-d-[4'linolenyl-6'-(tridecan-4"-one-1"-oxy)] Glucuranopyranoside (C66H110O8)	Stem bark (Khan et al., 2010)
77. Stigmast-5-en-3-*O*-β-d-glucopyranoside (C35H60O6)	Stem bark (Khan et al., 2010; Misra et al., 2008)
78. Sitosterol 3-*O*-β-d-glucopyranoside (C60H100O7)	Leaves (Kopa et al. 2014; Singh et al. 2010
79. Syringaresinol (C22H26O8)	Leaves (Lacret et al. 2012; Macias et al. 2008)
80. Medioresinol (C21H24O7)	Leaves (Lacret et al. 2012; Macias et al. 2008)
81. 1-Hydroxypinoresinol (C20H22O7)	Leaves (Lacret et al. 2012)
82. Lariciresinol (C20H24O6)	Leaves (Lacret et al. 2012; Macias et al. 2008)
83. Balaphonin (C20H20O6)	Leaves (Lacret et al. 2012)
84. Zhebeiresinol (C14H16O6)	Leaves (Lacret et al. 2012)
PHENYLPROPANOIDS : NORLIGNAN	
85. Tectonoelin A (C18H16O6)	Leaves (Lacret et al. 2012)

86. Tectonoelin B (C19H18O7)	Leaves (Lacret et al. 2012)
PHENYLETHANOID GLYCOSIDE	
87. Verbascoside or acteoside (C29H36O15)	Leaves (Singh et al. 2010)
FATTY ESTERS	
88. 7′-Hydroxy-n-octacosanoyl n-decanoate(C28H56O3	Stem bark (Khan et al. 2010)
89. 20′-Hydroxyeicosanyl linolenate (C38H72O3)	Stem bark (Khan et al. 2010)
90. 18′-Hydroxy-n-hexacosanyl-n-decanoate (C36H72O3)	Stem bark (Khan et al. 2010)
MISCELLANEOUS	
91. n-Docosane (C22H46) Stem bark	(Khan et al. 2010)
92. *O*-Tolylmethylether (C8H10O)	Wood (Lacret et al. 2012)

The docking investigation was completed for the ligands with the target protein Mpro (COVID–19 major protease) (PDB: 6LU7) by means of the docking software GLIDE, and the docked images of compound showing high docking score are given in Figs. 9.1 - 9.10. The Mpro in coronavirus is very important for the proteolytic maturation of the virus. Mpro has been examined as a potential target to prevent the spread of infection by inhibiting viral polyprotein cleavage through blocking active sites of the protein. (Figure 8). The active site in the protein 6LU7 consists of two chains; (i) small molecule- 02J (5-methylisoxasole–3-carboxylic acid) with PRO168 amino acid residue present in the active site. (ii) PJE-C–5-: composite ligand with THR26, VAL3, GLY143, SER144, HIS163, HIS164, GLU166 amino acid residues present in the active side. With this new discovery of Mpro structure in COVID–19, it has provided an immense opportunity to identify potential drug candidates for the treatment of coronavirus.

In molecular docking, the binding energy suggests the affinity of a specific ligand and strength by which a compound interacts with and binds to the pocket of a target protein. A compound with a lower binding energy is preferred as a possible drug candidate. In order to understand the effect of active antiviral and phytochemicals compounds on COVID–19. The structures docked by GLIDE are usually ranked according to the GLIDE scoring function (more negative). The scoring function of GLIDE docking program is offered in the G-score form. The most clear-cut method of evaluating the precision of a docking procedure is to determine how intimately the lowest energy pose (binding conformation) predicted by the object scoring function. To study the molecular basis of interaction and likeness of binding of ligands to COVID–19 Mpro, all the ligands were docked into the active site of COVID–19 Mpro. The docking result of these ligands is prearranged in Table 2.

Table 2: Glide score for the docked ligands

S. No.	Compound	Pubchem CID	Glide RMSD	Glide score
1	Barleriaquinone-I	155237	70.397	-7.723
2	Tectoquinone	6773	68.495	-6.895
3	Deoxylapachol	97448	69.848	-6.643
4	Quercitin	5280343	72.325	-6.507
5	Evofolin B	5317306	72.456	-6.446
6	Quinizarine	6688	73.316	-6.133
7	Munjistin	160476	70.822	-5.986
8	Grandiquinone A	102236728	73.347	-5.896
9	Lapachol	3884	69.426	-5.683
10	4-Methylquinoline	10285	69.386	-5.642
11	Rubiadin	124062	70.419	-5.559
12	Tecomaquinone-I	3574508	73.598	-5.521
13	Acetovanillone	2214	70.835	-5.404
14	Ellagic acid	5281855	72.292	-5.347
15	Annuionone a	72828705	69.007	-4.936
16	Tectol	161453	70.231	-4.325
17	Betulinaldehyde	99615	74.955	-4.271
18	Syringaresinol	100067	69.146	-4.205
19	Solidagonal acid	101285195	68.635	-4.198
20	Verbascoside	5281800	67.322	-4.12
21	Medioresinol	181681	70.315	-4.118
22	Phytol	5280435	69.141	-4.074
23	Lariciresinol	332427	66.907	-4.033
24	Rhinocerotinoic acid	11771531	71.253	-3.998
25	Lupeol	259846	73.759	-3.675
26	Betulinic acid	64971	73.34	-3.648
27	Rutin	5280805	67.847	-1.524

The interaction energy includes van der Waals energy, electrostatic energy, as well as intermolecular hydrogen bonding were calculated for each minimized complex. The docking score by means of GLIDE varied from −7.723 to −1.524 against COVID−19 major protease.

From the docking studies it is clear that all the compounds that are interacted at the active site of the COVID–19 Mpro (figure 10). All the compounds are thermodynamically feasible and shows significant glide score and they bind the hydrophobic pocket of the active site. The molecular docking analysis in the present study showed the inhibitory potential of 10 selected compounds, ranked by affinity (ΔG); Barleriaquinone-I > Tectoquinone > Deoxylapachol > Quercitin > Evofolin B > Quinizarine > Munjistin > Grandiquinone A > Lapachol > 4- Methylquinoline.

Lipinski's rule of five is a major criterion to evaluate drug likeliness and if a particular chemical compound with a certain biological and pharmacological activity has physical and chemical properties that would make it a likely orally active drug in humans. Lipinski's rule determines the molecular properties which are important for a drug's pharmacokinetics in the human body such as absorption, distribution, metabolism, and excretion (ADME). Lipinski's rule of five criteria for an ideal drug are (i) a molecular mass less than 500 Daltons, (ii) no more than 5 hydrogen bond donors, (iii) no more than 10 hydrogen bond acceptors, (iv) an octanol–water partition coefficient log P not greater than 5. Three or more than 3 violations do not fit into the criteria of drug likeliness and it is not considered in order to proceed with drug discovery. ADME studies of selected 27 compounds showed that out of 20 virtual hits were successful at passing through these ADME test filters (Table 3). This preliminary screening of potential molecules would help in providing the fast *in-silico* analysis towards development of therapeutics for COVID–19.

Due to technical limitations, Table 3 is provided in the Supplementary Files section.

The other targets for the selected compounds was done using SwissTargetPrediction method and it is based on the observation that similar bioactive molecules are more likely to share similar targets. Here the compounds showed high glide score for COVID–19 Mpro and also obeys the Lipinskis rule of five was selected for the prediction of other targets. From the analysis of Barleriaquinone-I it has an 30% probability with proteases enzyme target class among them most predicted target was Leukocyte elastase (figure 11) the other predicted targets with probability was given in the table 4. Table 5,6 and figure 11,12 shows the predicted targets for Tectoquinone and Deoxylapachol respectively. Tectoquinone targets phosphatases class and the most predicted target was dual specificity phosphatase Cdc25B were as Deoxylapachol targets Oxidoreductase class and predicted target was Monoamine oxidase B.

Table 4: Top 7 predicted targets and class for Barleriaquinone-I

Target	Common name	Uniprot ID	Target Class	Probability	Known actives (3D/2D)
Leukocyte elastase	ELANE	P08246	Protease	0.271400463	35/20
Estrogen receptor beta	ESR2	Q92731	Nuclear receptor	0.171518552	17/12
Estrogen receptor alpha	ESR1	P03372	Nuclear receptor	0.117056358	10/12
Serine/threonine-protein kinase PIM1	PIM1	P11309	Kinase	0.098947479	32/2
Casein kinase II alpha	CSNK2A1	P68400	Kinase	0.080792387	5/3
Protein-tyrosine phosphatase 4A3	PTP4A3	O75365	Phosphatase	0.071715932	1/1
Protein farnesyltransferase	FNTA FNTB	P49354 P49356	Enzyme	0.071715932	10/2

Table 5: Top 7 predicted targets and class for Tectoquinone

Target	Common name	Uniprot ID	Target Class	Probability	Known actives (3D/2D)
Dual specificity phosphatase Cdc25B	CDC25B	P30305	Phosphatase	0.075973634	11/5
Leukocyte elastase	ELANE	P08246	Protease	0.048952898	37/14
Acyl coenzyme A: cholesterol acyltransferase 1	SOAT1	P35610	Enzyme	0.048952898	5/0
P2X purinoceptor 7	P2RX7	Q99572	Ligand-gated ion channel	0.048952898	196/0
Dopamine D4 receptor	DRD4	P21917	Family A G protein-coupled receptor	0.048952898	24/0
Myeloperoxidase	MPO	P05164	Enzyme	0.048952898	14/0
Gamma-secretase	PSEN2	P49810	Protease	0.048952898	39/0

Table 6: Top 7 predicted targets and class for Deoxylapachol

Target	Common name	Uniprot ID	Target Class	Probability	Known actives (3D/2D)
Monoamine oxidase B	MAOB	P27338	Oxidoreductase	0.075973634	367/3
Indoleamine 2,3-dioxygenase	IDO1	P14902	Enzyme	0.075973634	30/12
G-protein coupled receptor 35	GPR35	Q9HC97	Family A G protein-coupled receptor	0.057956876	0/1
Dual specificity phosphatase Cdc25B	CDC25B	P30305	Phosphatase	0.057956876	20/13
P2X purinoceptor 7	P2RX7	Q99572	Ligand-gated ion channel	0.048952898	274/0
Monoamine oxidase A	MAOA	P21397	Oxidoreductase	0.048952898	158/2
Glutathione reductase	GSR	P00390	Oxidoreductase	0.048952898	4/4

4. Conclusion

The rate of COVID−19 infection in China is declining and new shocking outbreaks are emerging in Italy, Indonesia, South Korea, India, middle east and Europe, with a major risk for a pandemic situation. The scientific community is hence called for a collaborative and extraordinary effort for a rapid identification of an effective anti-COVID−19 drug. In this matter, we hope that our contribution through drug repurposing against target COVID−19 major protease of novel coronavirus (COVID−19) can be of great help in such a worldwide endeavor. In conclusion, we have a notorious molecules Barleriaquinone-I, Tectoquinone, Deoxylapachol, and Quercitin, an inventive drug candidate that was docked against COVID−19 major protease in a premeditated attempt to ascertain a new drug candidate, which is able to obstruct the diverse key target points of COVID−19 in treating novel corona virus. This compound Barleriaquinone-I, Tectoquinone, Deoxylapachol, and Quercitin well calculated as a best (lead) molecule and we necessitate design analogs, synthesis and evaluate its effectiveness against viral disease caused by COVID−19 through the molecular level and *in vivo* studies.

References

1. Agarwal, S.C., Sarngadharan, M.G., Seshadri, T.R., 1965. Colouring matter of teak leaves: isolation and constitution of tectoleafquinone. Tetrahedron Lett. 6, 2623–2626. https://doi.org/10.1016/S0040-4039(00)90218-1
2. Amudha, M., Rani, S., 2016. In silico molecular docking studies on the phytoconstituents of cadaba fruticosa (l.) Druce for its fertility activity. Asian J. Pharm. Clin. Res. 48–50.
3. Burnett, A.R., Thomson, R.H., 1968. Naturally occurring quinones. Part XV. Biogenesis of the anthraquinones in Rubia tinctorum L. (madder). J. Chem. Soc. C Org. 2437–2441.

https://doi.org/10.1039/J39680002437

4. Burnett, A.R., Thomson, R.H., 1967. Naturally occurring quinones. Part X. The quinonoid constituents of Tabebuia avellanedae(Bignoniaceae). J. Chem. Soc. C Org. 2100–2104. https://doi.org/10.1039/J39670002100
5. Chen, Y., Liu, Q., Guo, D., 2020. Emerging coronaviruses: Genome structure, replication, and pathogenesis. J. Med. Virol. 92, 418–423. https://doi.org/10.1002/jmv.25681
6. Chen, Y.W., Yiu, C.-P.B., Wong, K.-Y., 2020. Prediction of the SARS-CoV-2 (2019-nCoV) 3C- like protease (3CLpro) structure: virtual screening reveals velpatasvir, ledipasvir, and other drug repurposing F1000Research 9, 129. https://doi.org/10.12688/f1000research.22457.1
7. Cui, J., Li, F., Shi, Z.-L., 2019. Origin and evolution of pathogenic coronaviruses. Nat. Rev. 17, 181–192. https://doi.org/10.1038/s41579-018-0118-9
8. De Clercq, E., 2004. Antiviral drugs in current clinical use. J. Clin. Virol. Off. Publ. Pan Am. Soc. Virol. 30, 115–133. https://doi.org/10.1016/j.jcv.2004.02.009
9. Dhruva, b., br, d., av, r.r., r, s., k, v., 1972. Structure of a quinone from teak tissue culture. Struct. Quinone teak tissue Cult.
10. Ghosh, T., Chattopadhyay, K., Marschall, M., Karmakar, P., Mandal, P., Ray, B., 2009. Focus on antivirally active sulfated polysaccharides: from structure-activity analysis to clinical evaluation. Glycobiology 19, 2–15. https://doi.org/10.1093/glycob/cwn092
11. Gopal Samy, B., Xavier, L., 2015. Molecular Docking Studies on Antiviral Drugs for SARS. Int. Adv. Res. Comput. Sci. Softw. Eng. 5, 75–79.
12. Grinter, S.Z., Zou, X., 2014. Challenges, applications, and recent advances of protein-ligand docking in structure-based drug design. Mol. Basel Switz. 19, 10150–10176. https://doi.org/10.3390/molecules190710150
13. Gupta, p.k., singh, p., 2004. Note: a naphthoquinone derivative from tectona grandis (linn.). J. Asian Nat. Prod. Res. 6, 237–240. https://doi.org/10.1080/10286020310001653192
14. Gupta, K., Singh, P., 2004. A naphthoquinone derivative from Tectona grandis (Linn.). J. Asian Nat. Prod. Res. 6, 237–240. https://doi.org/10.1080/10286020310001653192
15. Hui, D.S., I Azhar, E., Madani, T.A., Ntoumi, F., Kock, R., Dar, O., Ippolito, G., Mchugh, T.D., Memish, Z.A., Drosten, C., Zumla, A., Petersen, E., 2020. The continuing 2019-nCoV epidemic threat of novel coronaviruses to global health - The latest 2019 novel coronavirus outbreak in Wuhan, Int. J. Infect. Dis. IJID Off. Publ. Int. Soc. Infect. Dis. 91, 264– 266. https://doi.org/10.1016/j.ijid.2020.01.009
16. Hupfeld, J., Efferth, T., 2009. Review. Drug resistance of human immunodeficiency virus and overcoming it by natural products. Vivo Athens Greece 23, 1–6.
17. Jayaprakasha, K., Jagan Mohan Rao, L., Sakariah, K.K., 2002. Improved HPLC Method for the Determination of Curcumin, Demethoxycurcumin, and Bisdemethoxycurcumin. J. Agric. Food Chem. 50, 3668–3672. https://doi.org/10.1021/jf025506a

18. Khan, R.M., Mlungwana, S.M. (Department of A.S., 1999. 5-Hydroxylapachol: a cytotoxic agent from Tectona grandis. Phytochem. U. K.
19. Khan, Z., Ali, M., Bagri, P., 2010. A new steroidal glycoside and fatty acid esters from the stem bark of Tectona grandis Linn. Nat. Prod. Res. 24, 1059–1068. https://doi.org/10.1080/14786410902951088
20. Kopa, T.K., Tchinda, A.T., Tala, M.F., Zofou, D., Jumbam, R., Wabo, H.K., Titanji, V.P.K., Frédérich, M., Tan, N.-H., Tane, P., 2014. Antiplasmodial anthraquinones and hemisynthetic derivatives from the leaves of Tectona grandis (Verbenaceae). Phytochem. Lett. 8, 41–45. https://doi.org/10.1016/j.phytol.2014.01.010
21. Krishna, C.J., Singh, P., Pardasani, R.T., 1977. Chemical components of the roots of Tectona grandis and Gmelina arborea. Planta Med. 32, 71–75. https://doi.org/10.1055/s-0028- 1097561
22. Lacret, , Varela, R.M., Molinillo, J.M.G., Nogueiras, C., Macías, F.A., 2011. Anthratectone and naphthotectone, two quinones from bioactive extracts of Tectona grandis. J. Chem. Ecol. 37, 1341–1348. https://doi.org/10.1007/s10886-011-0048-8
23. Lukmandaru, G., Takahashi, K., 2009. Radial distribution of quinones in plantation teak (Tectona grandis L.f.). Ann. For. Sci. 66, 605–605. https://doi.org/10.1051/forest/2009051
24. Macías, F.A., Lacret, R., Varela, R.M., Nogueiras, C., Molinillo, J.M.G., 2008. Bioactive apocarotenoids from Tectona grandis. Phytochemistry 69, 2708–2715. https://doi.org/10.1016/j.phytochem.2008.08.018
25. Martin, F.W., Service, U.S.F., Sidki), L.D. (Sadik, 1974. National Forest landscape management.
    1. Agricultural Research Service, U.S. Department of Agriculture.
26. Misra, L., Mishra, P., Pandey, A., Sangwan, R.S., Sangwan, N.S., Tuli, R., 2008. Withanolides from Withania somnifera roots. Phytochemistry 69, 1000–1004. https://doi.org/10.1016/j.phytochem.2007.10.024
27. Mounguengui, S., Saha Tchinda, J.-B., Ndikontar, M.K., Dumarçay, S., Attéké, C., Perrin, D., Gelhaye, E., Gérardin, P., 2016. Total phenolic and lignin contents, phytochemical screening, antioxidant and fungal inhibition properties of the heartwood extractives of ten Congo Basin tree Ann. For. Sci. 73, 287–296. https://doi.org/10.1007/s13595-015- 0514-5
28. Mukesh, B., Rakesh, K.Y., 2011. Molecular docking: a review [WWW Document]. URL https://www.semanticscholar.org/paper/molecular-docking%3a-a-review-Mukesh-Rakesh/65bacc6bf0191e2c4295748dbf091af371840284 (accessed 4.6.20).
29. Nayeem, N., Karvekar, 2010. Isolation of phenolic compounds from the methanolic extract of Tectona grandis. Res. J. Pharm. Biol. Chem. Sci. 1, 221–225.
30. Parasuraman, P., Swaminathan, S., Dhanaraj, P., 2014. Balancing anti-amyloid and anti-cholinesterase capacity in a single chemical entity: InSilico drug design. Int. J. Pharm. Pharm. Sci. 2, 571–574.
31. Paules, C.I., Marston, H.D., Fauci, A.S., 2020. Coronavirus Infections—More Than Just the Common Cold. JAMA 323, 707–708. https://doi.org/10.1001/jama.2020.0757

32. Prajapat, M., Sarma, P., Shekhar, N., Avti, P., Sinha, S., Kaur, H., Kumar, S., Bhattacharyya, A., Kumar, , Bansal, S., Medhi, B., 2020. Drug targets for corona virus: A systematic review. Indian J. Pharmacol. 52, 56–65. https://doi.org/10.4103/ijp.IJP_115_20
33. Rudman, P., 1960. Anthraquinones of Teak (Tectona grandis L.F.). Chem. Ind. 44, 1356–7.
34. Sandermann, W., Simatupang, M.H., 1966. Zur Chemie und Biochemie des Teakholzes (Tectona grandis L. fil). Holz Als Roh- Werkst. 24, 190–204. https://doi.org/10.1007/BF02610269
35. Singh, P., Jain, S., Bhargava, S., 1989. A 1,4-Anthraquinone derivative from Tectona grandis.Phytochemistry 28, 1258–1259. https://doi.org/10.1016/0031-9422(89)80224-9
36. Song, Z., Xu, Y., Bao, L., Zhang, L., Yu, P., Qu, Y., Zhu, H., Zhao, W., Han, Y., Qin, C., 2019. From SARS to MERS, Thrusting Coronaviruses into the Spotlight. Viruses 11. https://doi.org/10.3390/v11010059
37. St John, S.E., Tomar, S., Stauffer, S.R., Mesecar, A.D., 2015. Targeting zoonotic viruses: Structure-based inhibition of the 3C-like protease from bat coronavirus HKU4–The likely reservoir host to the human coronavirus that causes Middle East Respiratory Syndrome (MERS). Bioorg. Med. Chem. 23, 6036–6048. https://doi.org/10.1016/j.bmc.2015.06.039
38. Sumthong, P., Romero-González, R.R., Verpoorte, R., 2008. Identification of Anti-Wood Rot Compounds in Teak (Tectona grandis L.f.) Sawdust Extract. J. Wood Chem. Technol. 28, 247–260. https://doi.org/10.1080/02773810802452592
39. Thomson, R., 2012. Naturally Occurring Quinones. Elsevier.
40. Vyas, P., Yadav, D.K., Khandelwal, P., 2019. Tectona grandis (teak) – A review on its phytochemical and therapeutic potential. Nat. Prod. Res. 33, 2338–2354. https://doi.org/10.1080/14786419.2018.1440217
41. Windeisen, E., Klassen, A., Wegener, G., 2003. On the chemical characterisation of plantation teakwood from Panama. Holz Als Roh- Werkst. 61, 416–418. https://doi.org/10.1007/s00107-003-0425-2

Figures

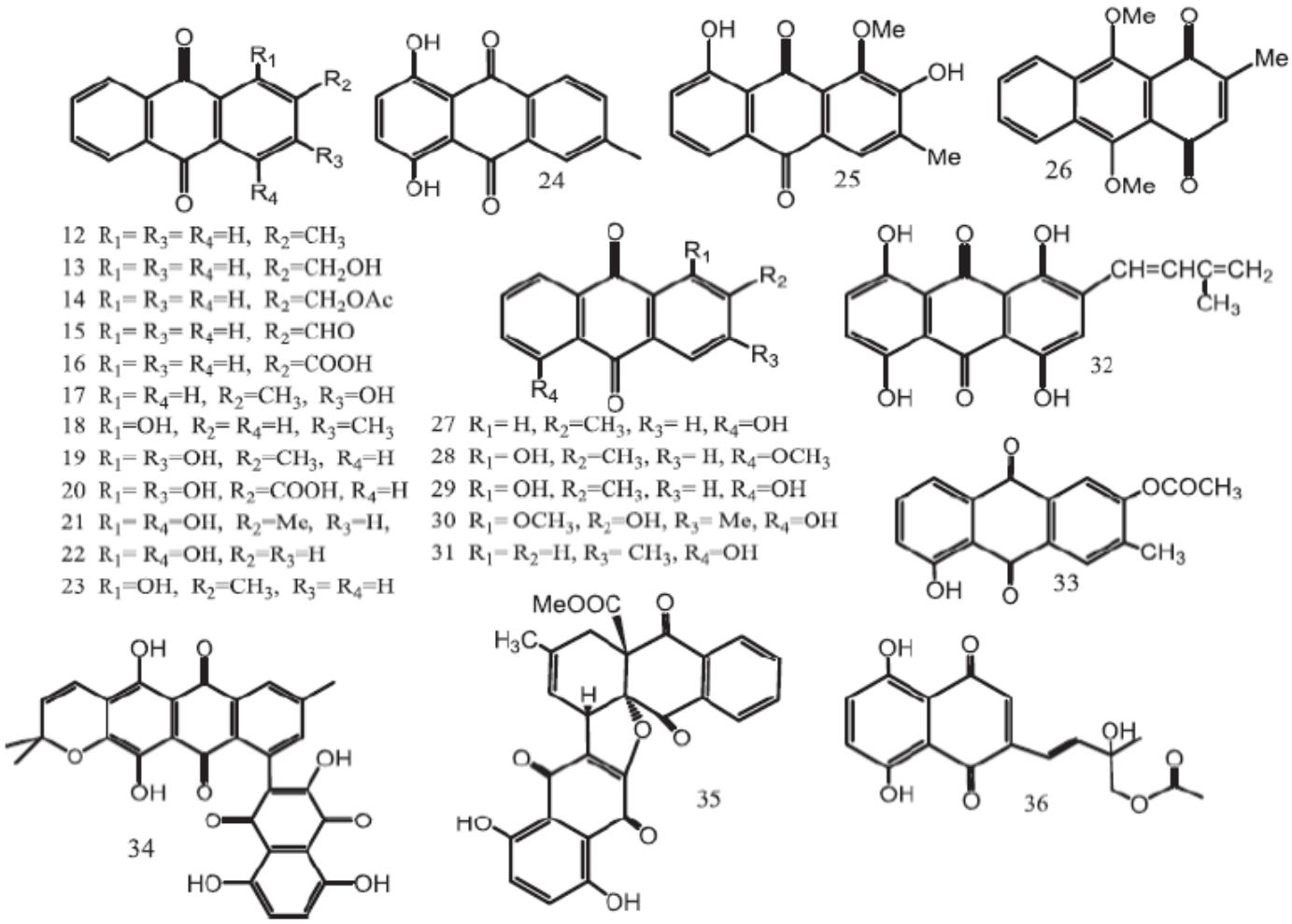

Figure 1

Chemical structures of anthraquinones.

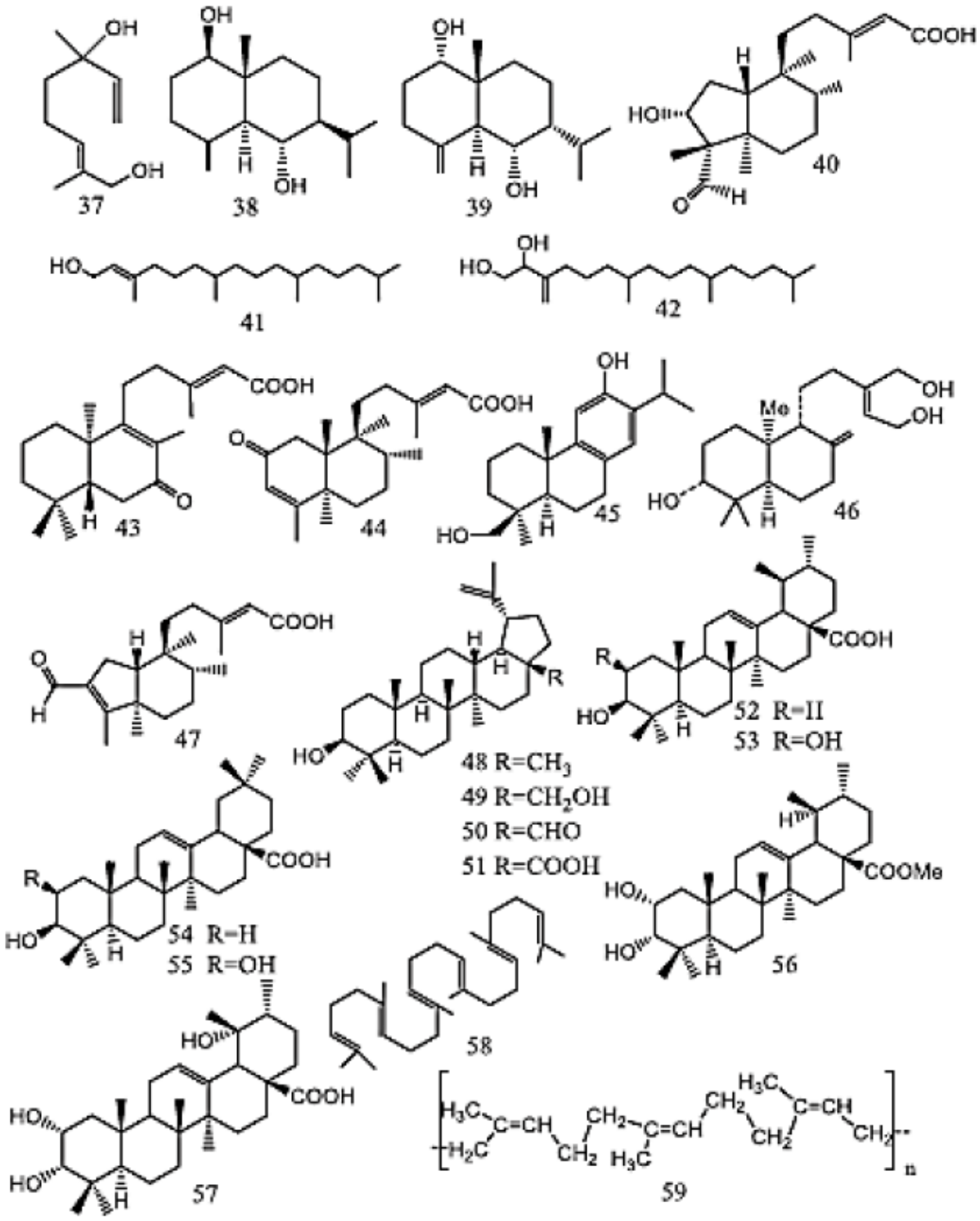

Figure 2

Chemical structures of terpenoids.

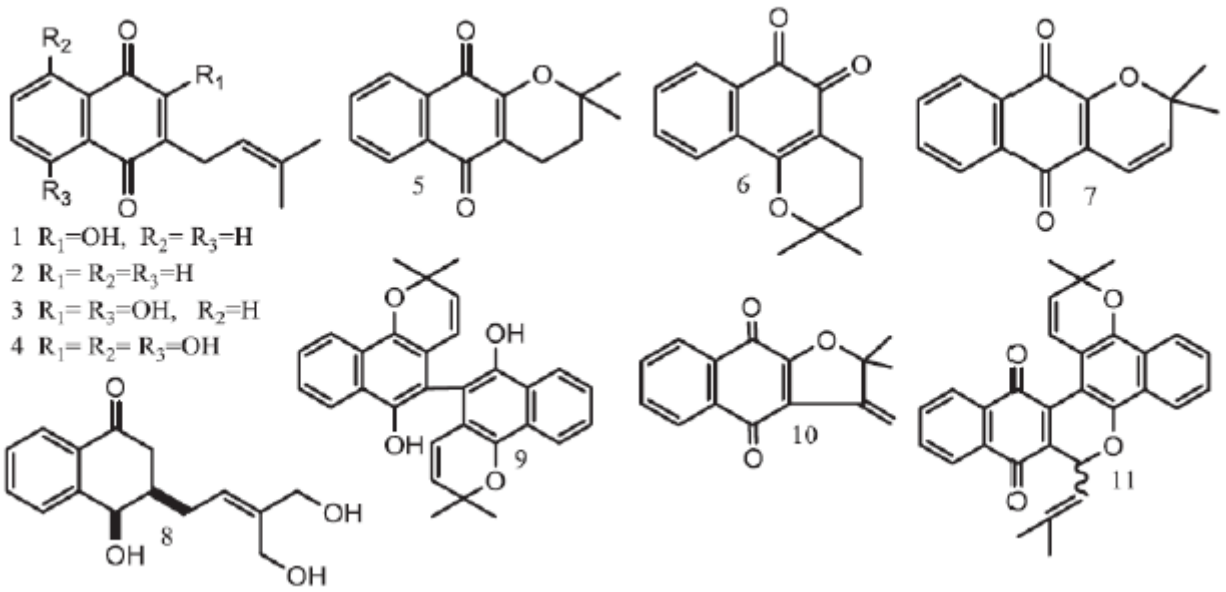

Figure 3

Chemical structures of naphthoquinones

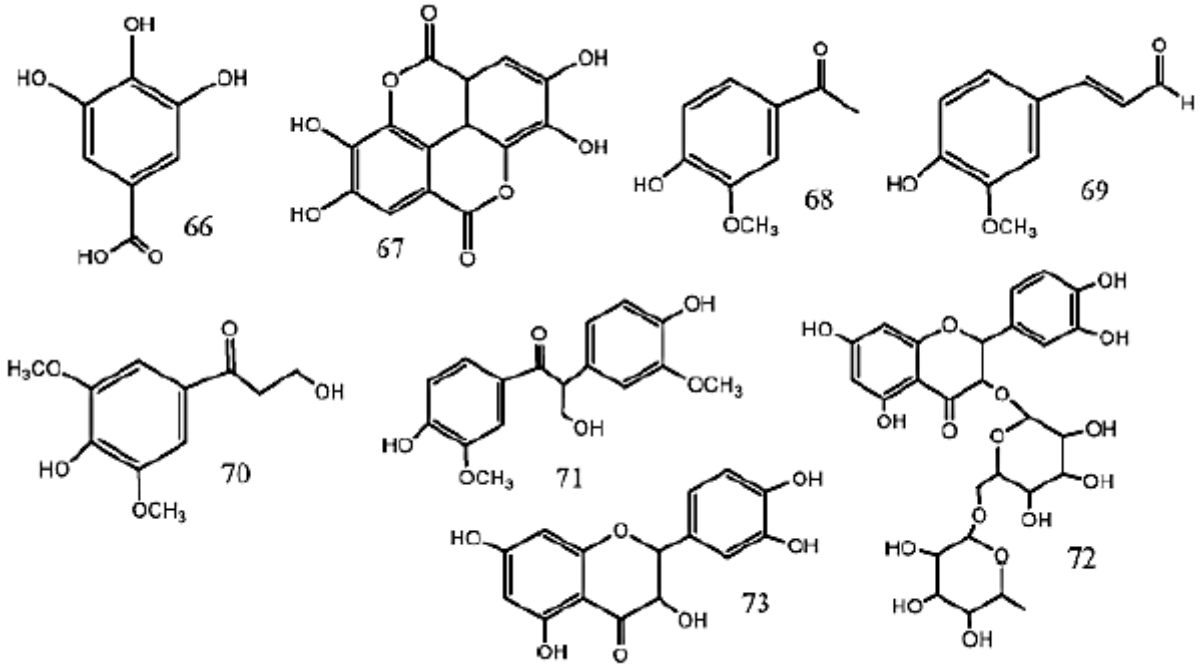

Figure 4

Chemical structures of phenolic compounds (66–71) and flavonoids (72–73).

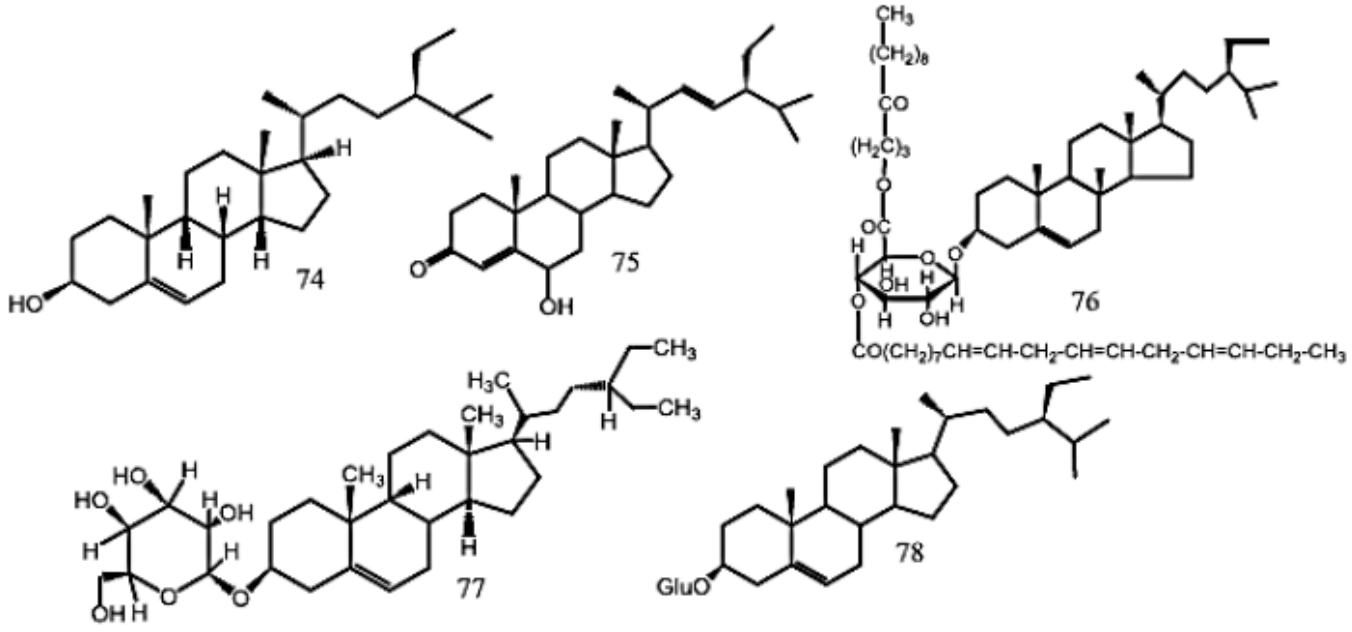

Figure 5

Chemical structures of streroids/saponins.

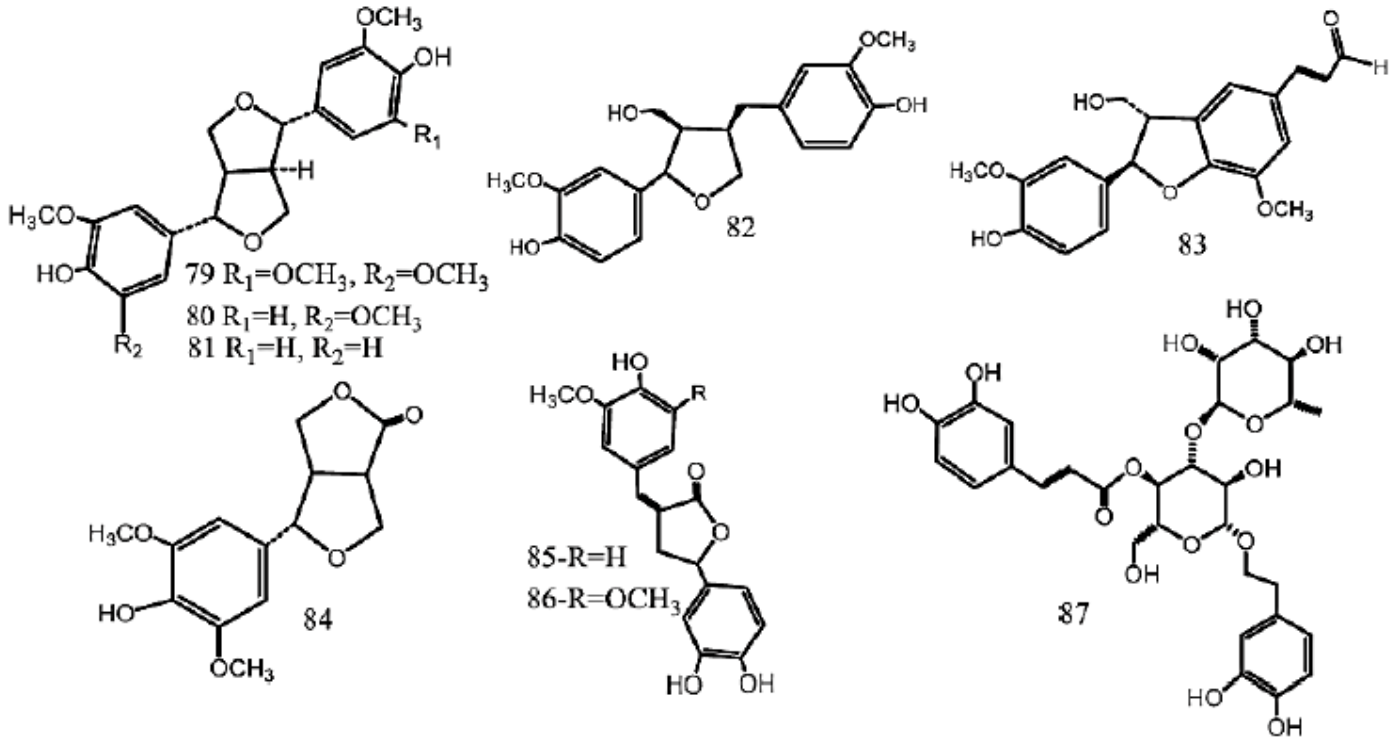

Figure 6

Chemical structures of phenylpropanoids (79–86) & phenylehtanoid glycoside (87).

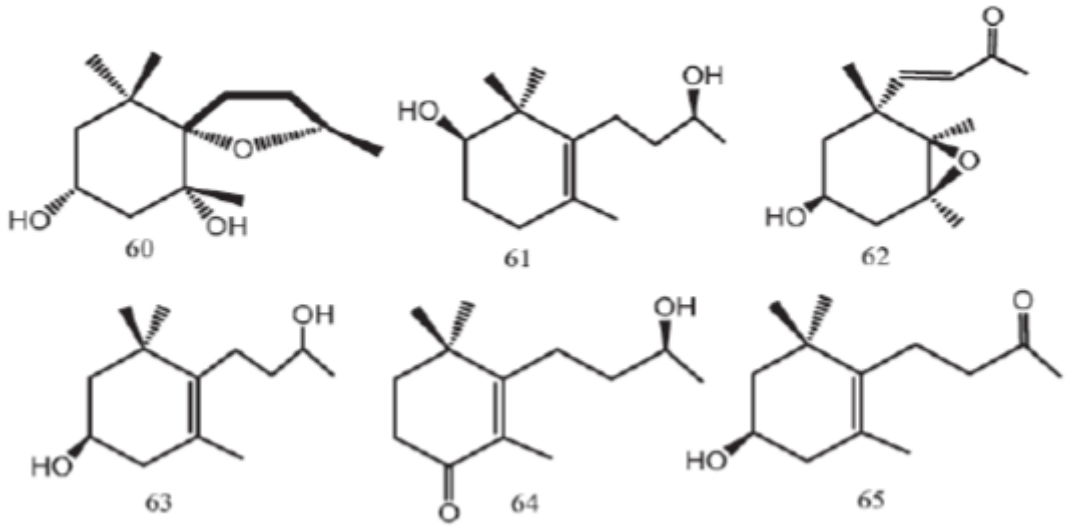

Figure 7

Chemical structures of apocarotenoids.

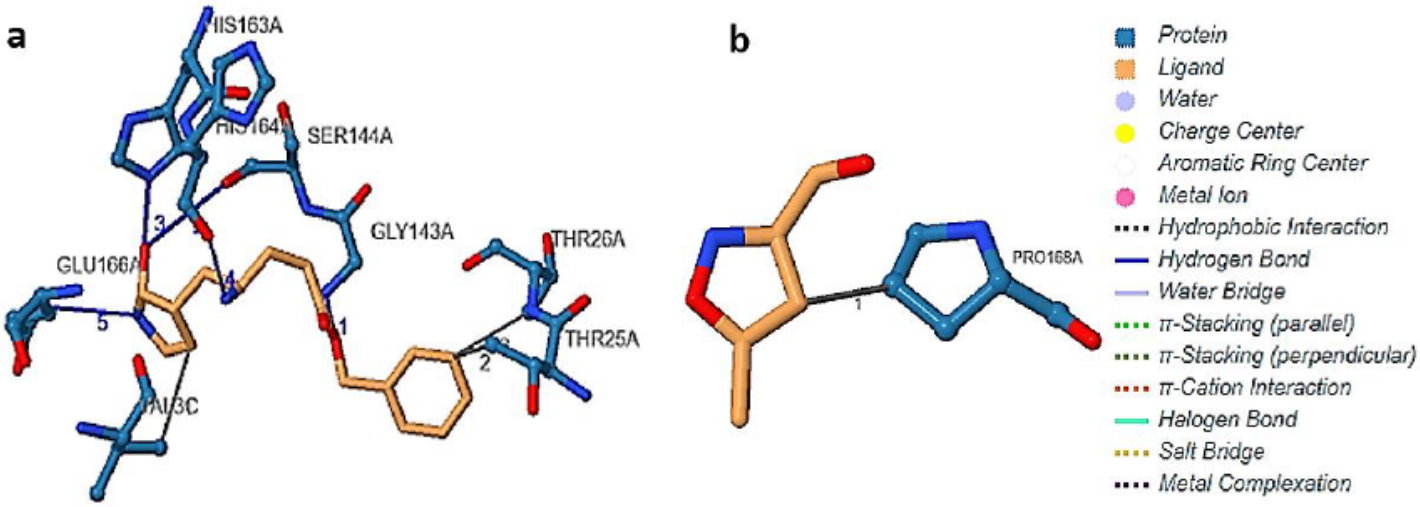

Figure 8

Represents the active sites (Ligand binding) in 6LU7. 6LU7 has 2 interacting chains. (a) Small molecule-02J (5methylisoxazole-3-carboxylic acid) interacting chain A (b) PJE (composite ligand) PJE- C-5 interacting chains A, C.

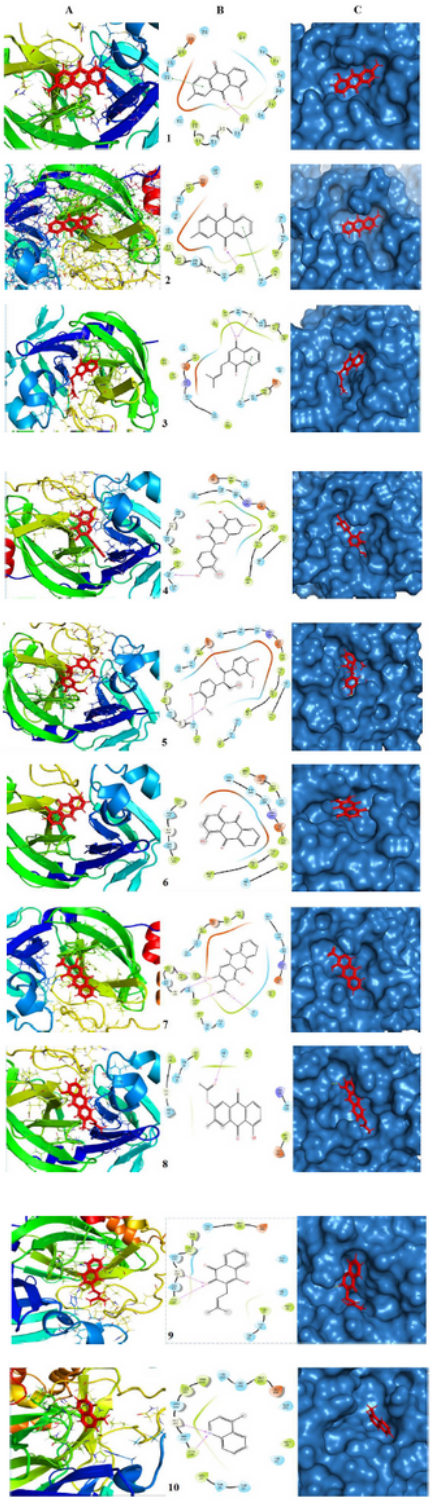

Figure 9

Molecular docking analysis between 6LU7 top 10 selected compounds from table 2.

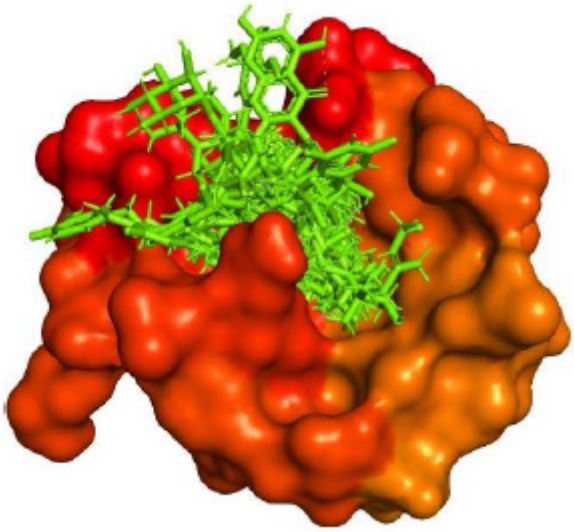

Figure 10

Interaction of selected compounds at the active site of COVID-19 Mpro

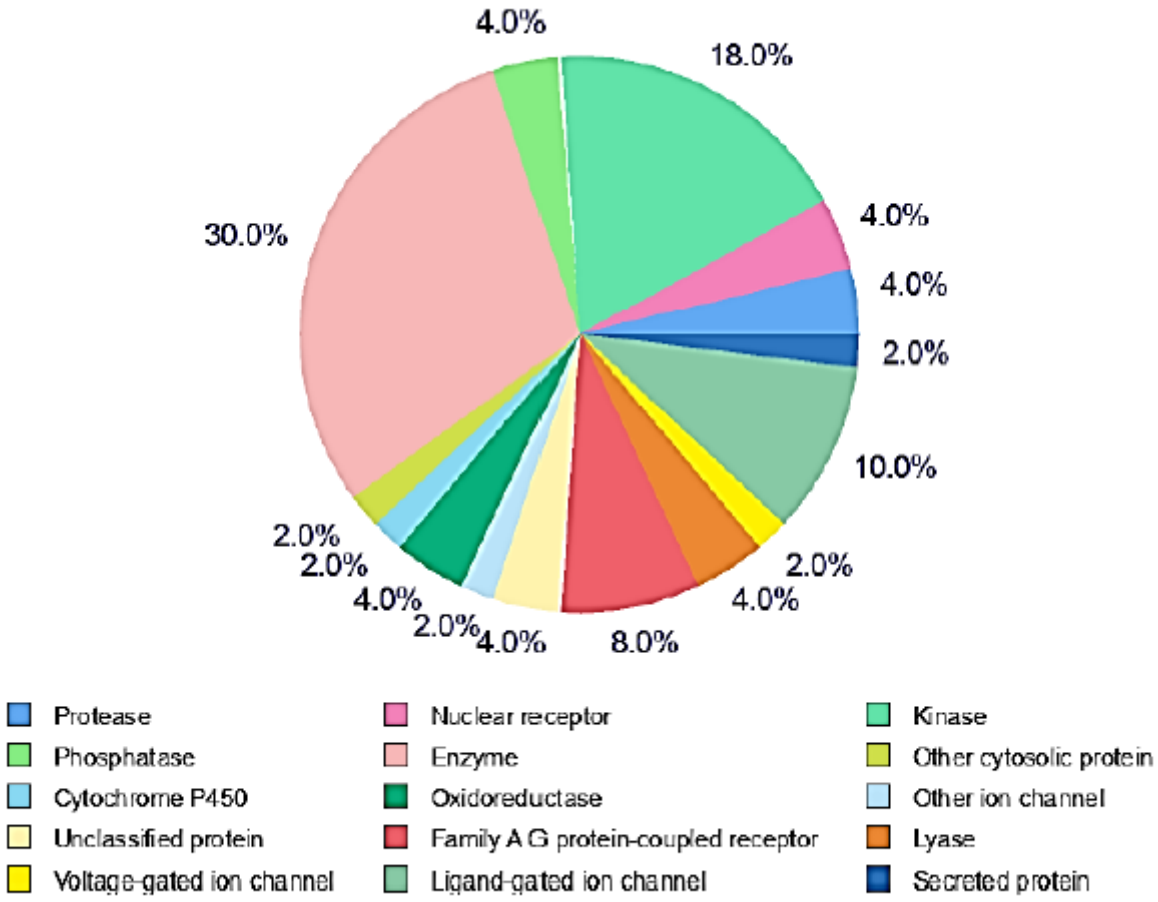

Figure 11

Predicted target group for Barleriaquinone-I

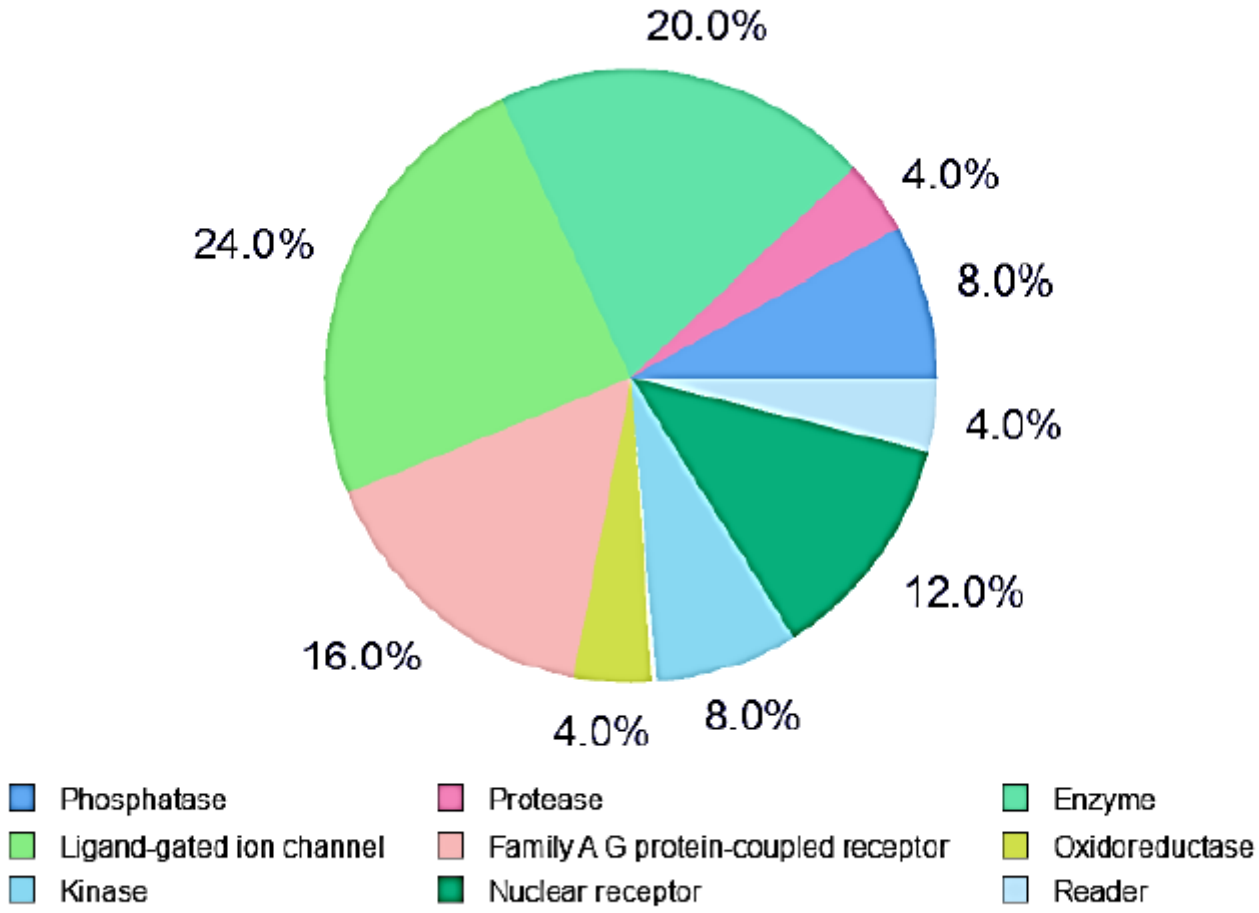

Figure 12

Predicted target group for Tectoquinone

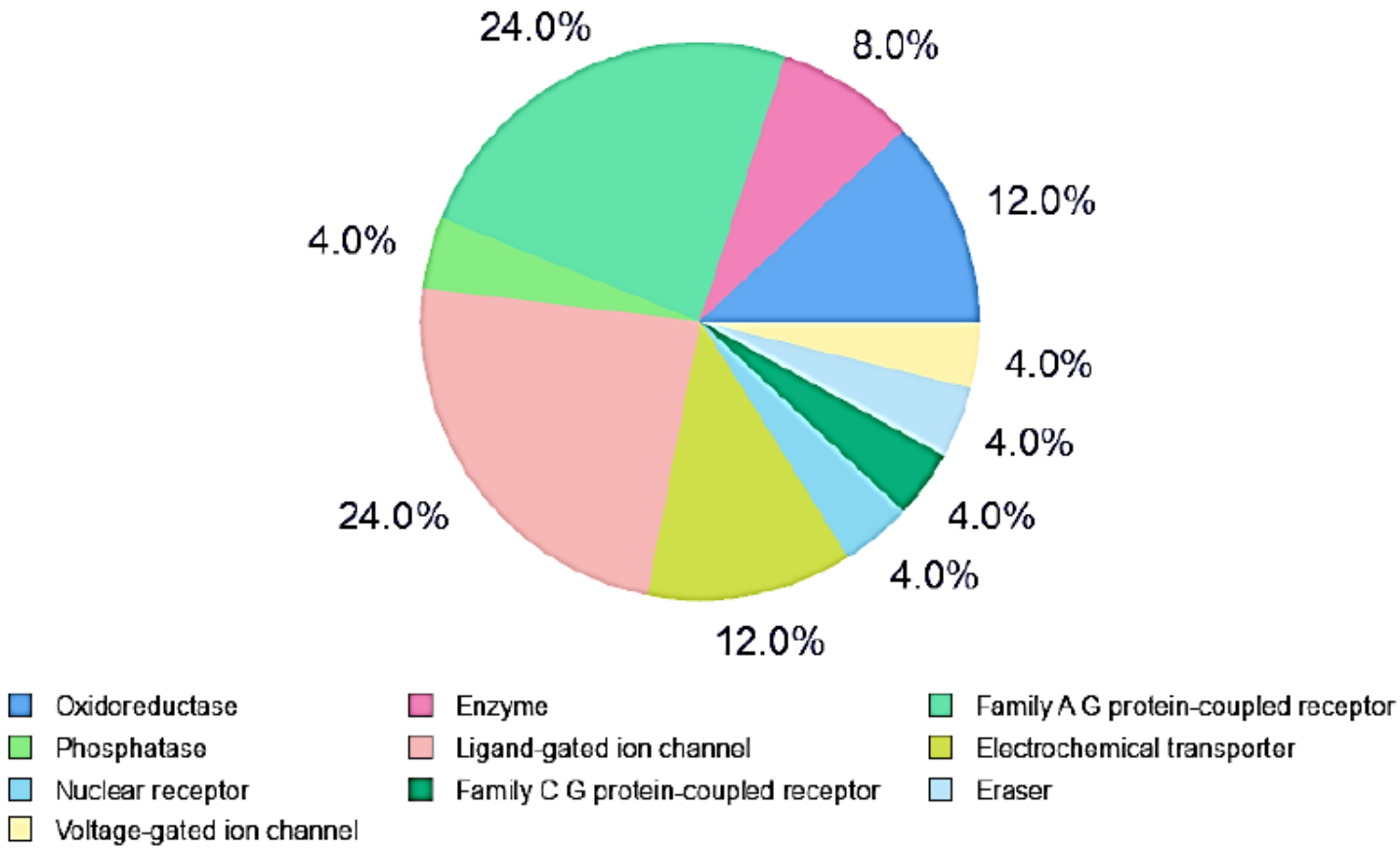

Figure 13

Predicted target group for Deoxylapachol

Supplementary Files

This is a list of supplementary files associated with this preprint. Click to download.

- Table3.docx